Available online at www.sciencedirect.com
SCIENCE DIRECT®
International Journal of Mass Spectrometry 228 (2003) 269–283
International Journal of Mass Spectrometry
www.elsevier.com/locate/ijms

A SIFT study of the reactions of H_3O^+, NO^+ and O_2^+ with hydrogen peroxide and peroxyacetic acid

P. Španěl[a,*], A.M. Diskin[b], T. Wang[b], D. Smith[b]

[a] *V. Čermák Laboratory, J. Heyrovský Institute of Physical Chemistry, Academy of Sciences of the Czech Republic, Dolejškova 3, 182 23, Prague 8, Czech Republic*

[b] *Centre for Science and Technology in Medicine, School of Postgraduate Medicine, Keele University, Thornburrow Drive, Hartshill, Stoke-on-Trent ST4 7QB, UK*

Received 13 December 2002; accepted 17 March 2003

Abstract

We have carried out a selected ion flow tube, SIFT, study of the reactions of H_3O^+, NO^+ and O_2^+ ions with hydrogen peroxide, H_2O_2, in the presence of excess water vapour and peroxyacetic acid, $CH_3C(O)OOH$, in the presence of comparable concentrations of acetic acid, CH_3COOH. This study was initiated to investigate if these peroxides could be analysed in humid air using selected ion flow tube mass spectrometry, SIFT-MS, using the above precursor ions. Rate coefficients and product ions have been determined for the NO^+ and O_2^+ reactions with H_2O_2 molecules (H_3O^+ ions do not react at a measurable rate with H_2O_2 molecules) and for the rapid reactions of H_3O^+, NO^+ and O_2^+ with $CH_3C(O)OOH$ molecules. It turns out that both H_3O^+ and O_2^+ ions are unsuitable for SIFT-MS analyses of these peroxides, either because of low reactivity and/or the production of common product ions for their reactions with H_2O and CH_3COOH molecules. However, the results of this study show that NO^+ precursor ions can be useful for the SIFT-MS analysis of both these peroxides, $NO^+H_2O_2$ being the monitor ion for hydrogen peroxide analysis in moist air, the production of this ion actually being catalysed by the presence of H_2O molecules, and NO_2^+ ion being suitable monitor ions for peroxyacetic acid analysis in the presence of acetic acid. The kinetic data for these peroxide reactions are presented and the likely mechanisms of the reactions are alluded to.

Keywords: SIFT; Hydrogen peroxide; Peroxyacetic acid; Ion–molecule reactions

1. Introduction

Peroxides as a class of compounds are extremely reactive, often unstable and are powerful oxidising agents. As such, studies of their reactions in the gas phase are challenging, see as an example, a study by Professor Helmut Schwarz and co-workers [1]. Thus, in celebration of the 60th birthday of Helmut, an outstanding scientist, stimulating speaker and good man of broad interests and high culture, we dedicate to him this paper on gas phase ion chemistry of peroxides.

Recently, in the development and applications of selected ion flow tube mass spectrometry, SIFT-MS, we have found the need to understand the ion chemistry of hydrogen peroxide, H_2O_2, in the gas phase, because it is known to be present in the exhaled breath and breath condensate of patients suffering from respiratory disease [2,3]. Also, the need has arisen to be able to detect and quantify peroxyacetic acid,

* Corresponding author. Tel.: +42-2-6605-2112; fax: +42-2-858-2307.
E-mail address: spanel@seznam.cz (P. Španěl).

1387-3806/$ – see front matter © 2003 Elsevier Science B.V. All rights reserved.
doi:10.1016/S1387-3806(03)00214-8

$CH_3C(O)OOH$, in air. This compound has major uses in sewage treatment, disinfecting [4], dialyser reuse [5] and industrial bleaching [6] (often as a commercial chlorine-free biodegradable disinfectant based on equilibrium mixtures of water, hydrogen peroxide, acetic acid and peroxyacetic acid [7]). Vapours of these chemicals are considered to be a potential health hazard [8] and are difficult to analyse using the widely used GCMS method. If the ion chemistry of these compounds with the precursor ions H_3O^+, NO^+ and O_2^+ (i.e., those available for chemical ionisation in the SIFT-MS analytical method) is understood, then SIFT-MS may be useful in the analysis of these peroxides. Whilst some ion chemistry of hydrogen peroxide and of its cation has been studied previously in order to understand their atmospheric chemistry [9], its detection by SIFT-MS has not been explored so far. Thus, we have carried out a selected ion flow tube study of the reactions of the H_3O^+, NO^+ and O_2^+ ions with H_2O_2 and $CH_3C(O)OOH$. This otherwise straightforward SIFT study is complicated because hydrogen peroxide cannot be totally isolated from water, so its ion chemistry has to be studied in parallel with that of water. Similarly, peroxyacetic acid can only be obtained as a mixture with acetic acid (with a small fraction of hydrogen peroxide) and so its ion chemistry must be inferred from that of a mixture of these two acids. Fortunately, however, the separate ion chemistries of water and acetic acid with H_3O^+, NO^+ and O_2^+ are well understood from previous SIFT studies [10,11]. In any event, the ion chemistries of water and acetic acid can be quickly studied alongside those of the hydrogen peroxide/water and the acetic acid/peroxyacetic acid mixtures respectively, to assist in the proper identification of the kinetics and ion products of the peroxide reactions.

2. Experimental

The standard SIFT technique has been described in numerous publications [12–14] and so it is sufficient here to state the following. The precursor ions H_3O^+, NO^+ and O_2^+ are generated in a discharge ion source and mass selected by a quadrupole mass filter before being injected as separate species into fast-flowing helium carrier gas in a flow tube. The reactant gases of interest are then introduced at controlled flow rates into the ion swarm/carrier gas where they react with the chosen precursor ion species. The loss rates of the precursor ions and the product ions of the reactions are determined by a downstream quadrupole mass spectrometer. This can be operated either in the full scan mode (FSM) over a predetermined m/z range to obtain a spectrum of the reactant and product ions or in the multi-ion mode (MIM) in which the spectrometer is switched and dwells on selected reactant/product ions as their count rates are determined [15]. The FSM is primarily used to identify the product ions and the MIM is used to determine product ion distributions more accurately.

In these studies, we have used two methods for introducing the vapours of the liquid reactants into the carrier gas as follows. One method involves the introduction of a drop of the liquid (or liquid mixture) into a sealable plastic bag, which is then inflated using dry cylinder air (to a volume of about 500 mL). The liquid vapour/air mixture is then introduced into the helium carrier gas via a variable leak (needle valve) and a flow meter by puncturing the bag with a hypodermic needle connected to the inlet port of the instrument. The rate coefficients and the product ion distributions are determined from the count rates of the precursor and product ions recorded as the flow of the reactant mixture is varied. Normally, the concentration of the liquid vapour in the air is unknown, so to determine the rate coefficients we compare the decay rates of the H_3O^+, NO^+ and O_2^+ ions, simultaneously injected into the carrier gas, as the dry air/sample flow rate is varied. Details of this technique have been given in several papers [13,14,16]. This particular method has been used exclusively for the acetic acid/peroxyacetic acid studies. How the ion chemistry of the peroxyacetic acid is derived from the total ion chemistry of the acetic acid/peroxyacetic acid mixture is explained later.

The second method involves puncturing a septum sealing a glass vessel (volume 150 mL) that contains the liquid sample and dry air (initially at atmospheric

pressure) with a hypodermic needle connected directly to the input port of the SIFT-MS instrument via a calibrated capillary. Then the headspace above the liquid is sampled directly into the carrier gas/ion swarm. As the sampling proceeds, the pressure in the sealed glass vessel decreases and this must be taken into account for accurate quantification. This phenomenon has been dealt with in detail in a recent publication [17]. This method of sample introduction has been useful in the water/hydrogen peroxide studies, as we explain later. To prevent condensation of water vapour onto the capillary/inlet lines, they are heated to about 100 °C. To vary the flow of water vapour and hydrogen peroxide into the carrier gas, the bottle/liquid sample temperature can be varied using a thermostatically controlled water bath. All the present studies were carried out at a helium carrier gas pressure of 0.7 Torr at room temperature (296–300 K).

3. Results

3.1. Hydrogen peroxide

For these experiments, we used a solution of hydrogen peroxide in water at a concentration of 50% by weight. This results in a partial pressure of H_2O_2 above the liquid of only a few percent of that of water vapour within the temperature range of interest, as can be seen in Fig. 1. Also, the presence of the H_2O_2 at this concentration in the mixture suppresses the water vapour pressure well below that for pure water at the same temperature, as can also be seen in Fig. 1. The relatively low vapour pressure [18] of the hydrogen peroxide (and the consequential low flow rates relative to water vapour) complicates the interpretation of the data and the accuracy of the derived rate coefficients. Nevertheless, in any real situation that we are likely to meet that requires the detection and quantification of H_2O_2 by SIFT-MS, water vapour will be present at greater concentration and so it is important to understand the ion chemistry occurring in the presence of water vapour.

3.1.1. H_3O^+ reactions

The initial experiments were performed by introducing about 1 mL of the water/hydrogen peroxide mixture into a plastic bag, which was then inflated with dry cylinder air to a volume of about 500 mL. The air/water vapour/gaseous hydrogen peroxide mixture (equilibrated at room temperature) was then introduced into the helium carrier gas via the variable

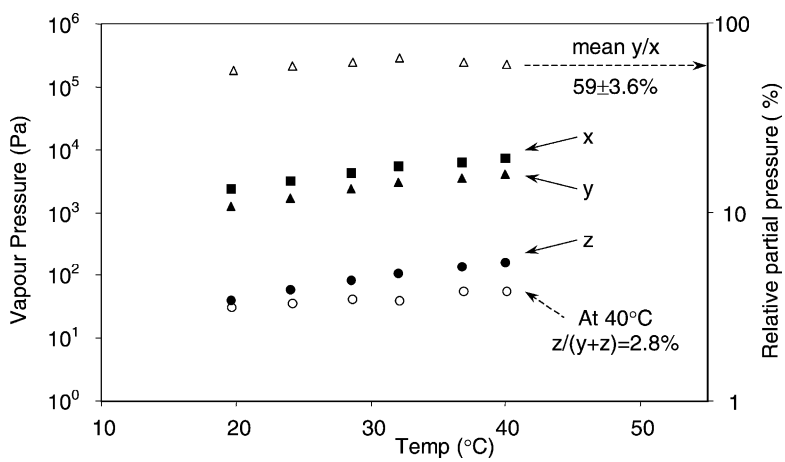

Fig. 1. The partial pressures of water vapour and hydrogen peroxide (H_2O_2) in Pascal (Pa), in the headspace of pure water and in a 50% (by weight) aqueous solution of H_2O_2 as a function of the liquid temperature. *x*, the partial pressure of H_2O in the headspace of pure water, *y*, the partial pressure of H_2O in the headspace of the water/peroxide solution and *z*, the partial pressure of H_2O_2 in the headspace of the water/peroxide solution. Also shown are the ratios of y/x and $z/(y+z)$ expressed as percentages. Data are taken from [18,25].

leak. A FSM spectrum was then obtained over an appropriate *m/z* range (typically 10–100) using H_3O^+ precursor ions to identify the products of any reactions that occurred. An identical experiment was performed using 1 mL of pure water in the bag. The only significant ions on the resulting FSM spectra in both experiments were the H_3O^+ ions and their hydrates, $H_3O^+(H_2O)_{1–3}$ at *m/z* values of 37, 55 and 73 (and a small fraction of 91) that are formed in sequential three-body association reactions [19] such as:

$$H_3O^+ + H_2O + He \rightarrow H_3O^+H_2O + He \quad (1)$$

However, there was an obvious difference between the distributions of these four ionic species when formed by air/water and the air/water/peroxide mixtures introduced at the same flow rates into the helium. The distributions were such that the larger clusters were not so abundant when the water/peroxide mixture was introduced, implying that less water vapour was being introduced. No ions were present with *m/z* values appropriate to cluster ions like $H_3O^+(H_2O)_m(H_2O_2)_n$, implying that H_2O_2 molecules do not react with H_3O^+ and its hydrates at observable rates. However, on a cautionary note, it must be remembered that the fraction of H_2O_2 molecules in the carrier gas is just a few percent of the H_2O molecules, so if mixed cluster ions do form they *may* react with the abundant H_2O molecules producing the $H_3O^+(H_2O)_{1–3}$ ions.

Experiments were then carried out in which the headspace of both air/water and air/water/peroxide in bottles (as described above) were sampled alternately at several fixed temperatures using the water bath. The distributions of the $H_3O^+(H_2O)_{0–3}$ ions were determined using the MIM mode of data acquisition and these are shown in Fig. 2 for liquid sample (bath) temperatures of 20, 24, 28, 32, 36 and 40 °C. Note the greater development of the higher-order clusters when the headspace from the bottles containing only pure water is introduced into the helium at each temperature. Note also the derived water vapour pressures in the sealed bottles in the case of the water alone and of the water/peroxide mixture at each temperature. We have described the method by which the water vapour pressure is derived in the carrier gas and in the air (bottle) sample in a previous paper [17]. As can be seen in Fig. 2, the ratio (percentage) of the measured water vapour pressures above the water/peroxide mixture (*y*) to that measured above the pure water (*x*) does not vary greatly over the temperature range 20–40 °C and is in accordance with expectations based on the data given in Fig. 1. Within the constraints of the small fractions of H_2O_2 to H_2O molecules, these collected data indicate that H_2O_2 does not react with H_3O^+ ions at a significant rate. It is known that the proton affinity of H_2O_2 (PA = 674.5 kJ mol^{-1}) is less than the PA of H_2O (691 kJ mol^{-1}) [20] and so the proton transfer reaction:

$$H_3O^+ + H_2O_2 \rightarrow H_2O_2H^+ + H_2O \quad (2)$$

is sufficiently endothermic to prevent reaction at 300 K.

3.1.2. O_2^+ reactions

It is well known that ground state O_2^+ ions do not undergo bimolecular reaction with H_2O molecules, but rather slow three-body association occurs at thermal energy [21]:

$$O_2^+ + H_2O + He \rightarrow O_2^+H_2O + He \quad (3)$$

By virtue of the ionisation energy of H_2O (IE = 12.62 eV) and the recombination energy of O_2^+ (RE = 12.07 eV) [22], charge transfer between O_2^+ and H_2O is endothermic. However, the IE of H_2O_2 (=10.58 eV) [22] is relatively low, and thus, the following bimolecular charge transfer reaction is exothermic and can proceed at thermal energy (although this is no guarantee that the reaction will be fast [9]):

$$O_2^+ + H_2O_2 \rightarrow H_2O_2^+ + O_2 \quad (4)$$

The experiments described above using H_3O^+ precursor ions were repeated using O_2^+ precursor ions. For water vapour only, as expected, a minor product ion at *m/z* of 50 (i.e., $O_2^+H_2O$) was seen in the FSM spectra and the major product ions were $H_3O^+(H_2O)_{0–3}$. It is well known, especially in relation to atmospheric ion chemistry [23], that the $O_2^+(H_2O)_{1,2}$ hydrated ions react with H_2O molecules ultimately to generate hydrated hydronium ions and

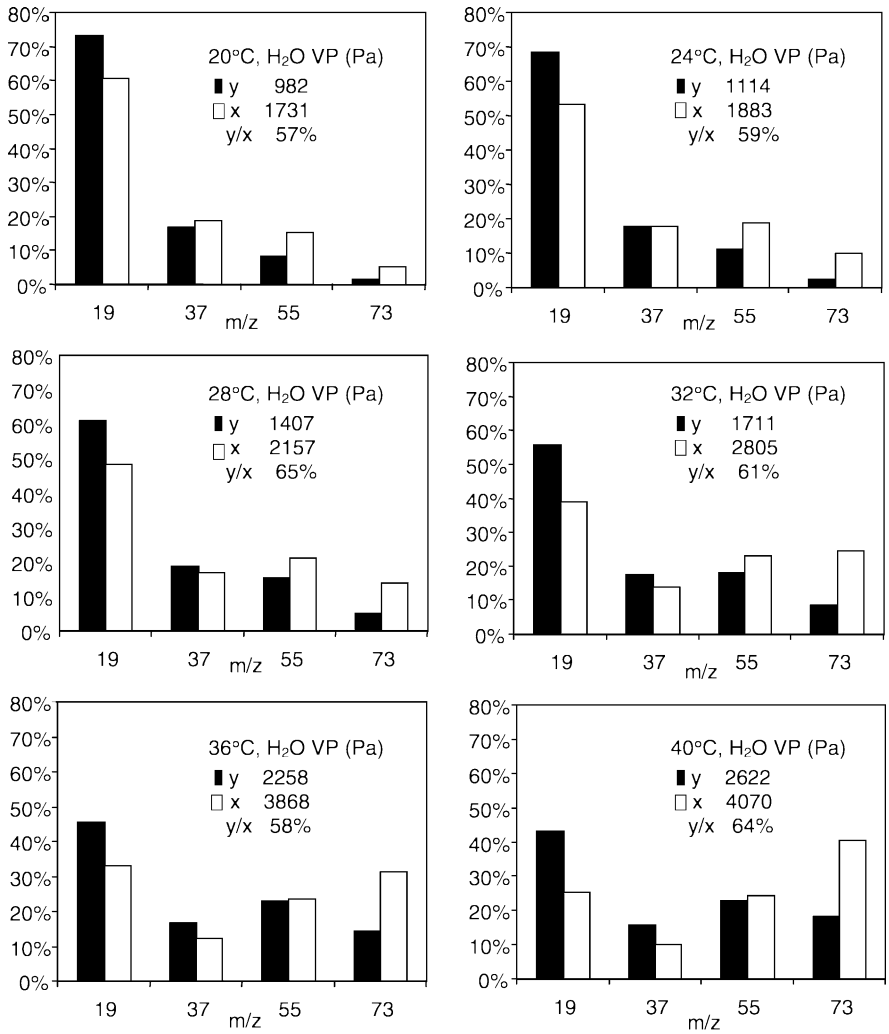

Fig. 2. Distributions of the $H_3O^+(H_2O)_{0–3}$ ions formed in the SIFT using H_3O^+ precursor ions when the headspace above 10 mL liquid samples in sealed glass bottles (volume 150 mL) at the temperatures indicated is introduced into the carrier gas at the same flow rate. *x*, open bars, the air/vapour headspace above pure water. *y*, filled bars, the air/vapour headspace above a mixture of 50% by weight of H_2O_2 in water. Also shown are the ratios of the water vapour partial pressure, VP, above the two different liquids, *y*/*x*, expressed as percentages (%).

this ion chemistry is the major route to these ions observed in these SIFT experiments. However, it should be noted that a small percentage of the O_2^+ ions formed in the discharge ion source are electronically excited and these are able to retain their excitation energy in the helium carrier gas and then react rapidly with H_2O molecules ultimately contributing to the observed $H_3O^+(H_2O)_{0–3}$ ions.

The addition of the water/peroxide vapour to the carrier gas results in a major loss of O_2^+ ions and a concomitant production of H_3O^+ and its hydrates. Controlled experiments were carried out using both water and water/peroxide samples in bottles (as described above) at different temperatures using the water bath. Sample data are shown in Fig. 3. Note the reduction in the O_2^+ percentage as the temperature

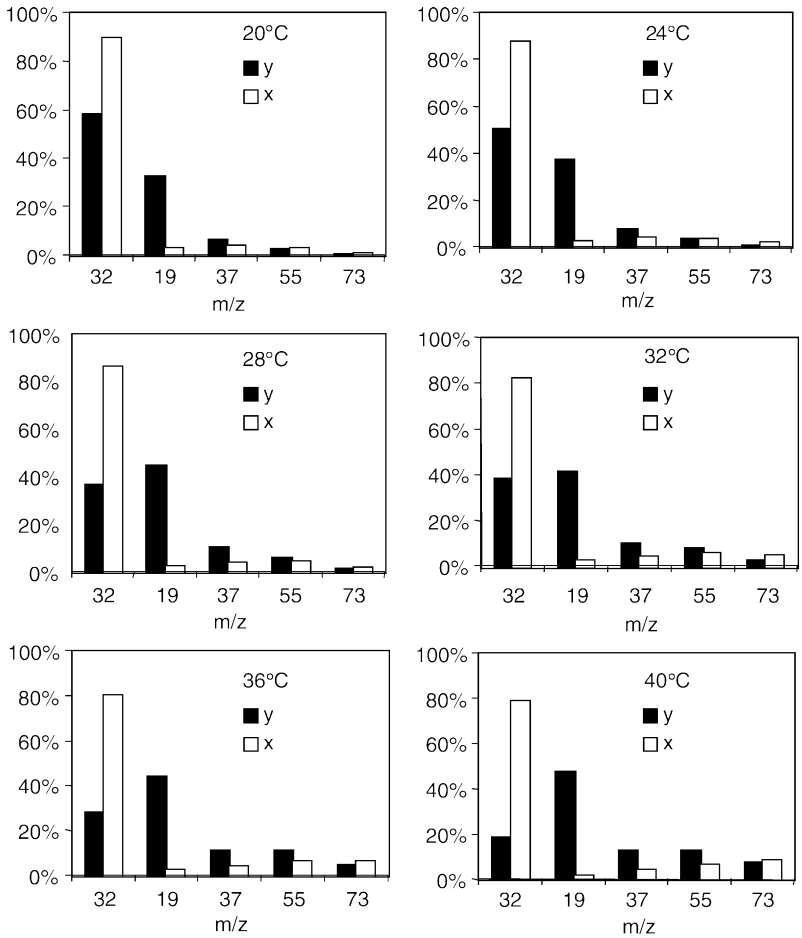

Fig. 3. Distributions of the $H_3O^+(H_2O)_{0–3}$ ions formed in the SIFT and the varying O_2^+ precursor ion signals when the headspace above 10 mL liquid samples in sealed glass bottles (volume 150 mL) at the temperatures indicated is introduced into the carrier gas at the same flow rate. *x*, open bars, the air/vapour headspace above pure water, *y*, filled bars, the air/vapour headspace above a mixture of 50% by weight of H_2O_2 in water. Note the reduction in the O_2^+ signal as the temperature of the water/peroxide mixture is increased, and thus as the flows of water vapour and hydrogen peroxide into the carrier gas increases. Note, also, that the higher-order H_3O^+ hydrates are less abundant when the water/hydrogen peroxide mixture is sampled, because less water is being introduced (see Figs. 1 and 2).

of the water/peroxide mixture is increased, and thus as the flows of water vapour and hydrogen peroxide into the carrier gas increase. Note, also that the higher-order H_3O^+ hydrates are not so well represented on the distributions that result when the water/peroxide mixture is used. This is simply because less water is being introduced (see the previous section and Figs. 1 and 2). These data indicate that O_2^+ ions react rapidly with H_2O_2 molecules, presumably via the charge transfer reaction (4). The proof of this is that the product ion signal at the *m*/*z* value of 34 increases with increasing water/peroxide sample flow, showing that $H_2O_2^+$ ions are being produced (see Fig. 4b).

To determine the rate coefficient for reaction (4), measurements were made of the decay rates of the $^{16}O^{16}O^+$ ions at *m*/*z* of 32 as a function of the H_2O_2 flow rate. The latter is obtained from the flow rate of the air/water vapour/peroxide mixture (as determined using the flow meter) and the known partial pressure of the H_2O_2 in the mixture obtained from Fig. 1. A

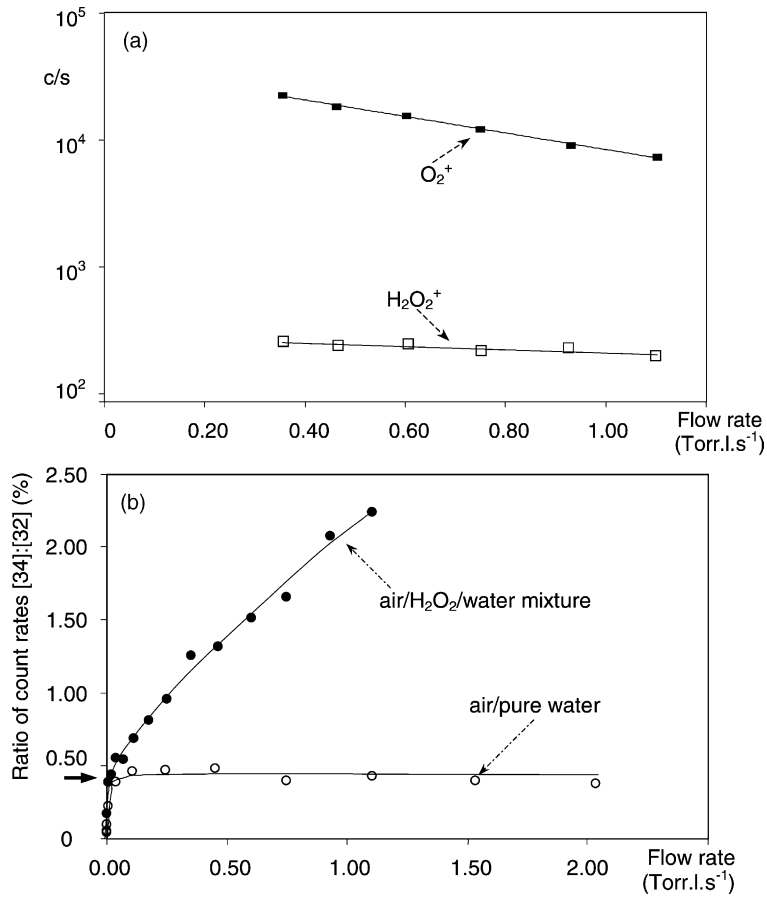

Fig. 4. (a) A semilogarithmic plot of the O_2^+ precursor ion count rates (counts per second, c/s) as a function of flow rate (Torr L s^{-1}) of the air/vapour headspace from a solution of H_2O_2 (50% by weight) in water. The slope of this decay plot provides the rate coefficient for reaction (4). Also shown are the product ion $H_2O_2^+$ count rates obtained by subtracting the 0.4% $^{16}O^{18}O^+$ isotopomer contribution to the ion signal at $m/z = 34$. (b) Ratios of count rates [34]/[32] (in percent, %) of ions at $m/z = 34$ to the O_2^+ precursor ion count rate at $m/z = 32$ as a function of the flow rate (Torr L s^{-1}) of headspace of the air/H_2O_2/water mixture (solid symbols) and air/pure water (open symbols). In the case of pure water, the ions at $m/z = 34$ are exclusively the $^{16}O^{18}O^+$ isotopomer ions. In the case of H_2O_2/water mixture, the ions at $m/z = 34$ comprise $^{16}O^{18}O^+$ and $H_2O_2^+$ formed in reaction (4). The arrow indicates the natural abundance of the ^{18}O isotope in O_2 molecules.

sample decay curve is shown in Fig. 4a. The value obtained for the rate coefficient is 2.0×10^{-9} cm^3 s^{-1} at 300 K. This is 25% lower than the calculated collisional rate coefficient of 2.7×10^{-9} cm^3 s^{-1} calculated using the parameterised trajectory calculation [24] and the polarisability and dipole moment of H_2O_2 [25], but 25% greater than the previous experimental value of 1.5×10^{-9} cm^3 s^{-1} [9]. In view of the uncertainty in the partial pressure of H_2O_2 above the water/peroxide mixture [18], there is a correspondingly greater uncertainty in the derived rate coefficient, which we estimate to be ±20%. Even so, the rate coefficient for reaction (4) is still lower than collisional, but this is not uncommon for charge transfer reactions involving small neutral reactant molecules [21].

Referring to Fig. 4b, it can be seen that at zero air/water/peroxide sample flow rate the ions at m/z of 34, which comprise $^{16}O^{18}O^+$ isotopomer ions and $H_2{}^{16}O_2^+$ product ions of the reaction (4), are just a tiny percentage of the ions at $m/z = 32$. However, for

a small flow of air/water/peroxide sample it reaches 0.4%. This is explained by the fact that the injected $m/z = 32$ ions consist of only $^{16}O^{16}O^+$ isotopomer ions, but with the introduction of a small amount of oxygen (air) the following rapid isotope exchange reaction occurs [26]:

$$^{16}O^{16}O^+ + {}^{16}O^{18}O \rightarrow {}^{16}O^{18}O^+ + {}^{16}O^{16}O \quad (5)$$

This reaction randomises the ^{16}O and ^{18}O isotopes in the ions towards the naturally occurring $^{18}O^{16}O$ isotopic ratio, which is 0.4% for the O_2 molecule [27]. The increase above 0.4% with increasing sample flow is due to the production of $H_2O_2{}^+$ ions by reaction (4). However, as can be seen in Fig. 4b, the ions at m/z of 34 never exceed about 2–3% of the signal at m/z of 32, i.e., of the $^{16}O^{16}O^+$ isotopomer ions, the signal of which decreases by more than a factor of two (see Fig. 4a). This indicates that the product $H_2O_2{}^+$ ions are being lost almost as fast as they are being formed. They are surely lost via exothermic proton transfer with the abundant H_2O molecules, thus:

$$H_2O_2{}^+ + H_2O \rightarrow H_3O^+ + HO_2 \quad (6)$$

The rate coefficient for this reaction can be obtained by considering the known production rate (by reaction (4)) and the loss rate (by reaction (6)) of the $H_2O_2{}^+$ ions. In the steady state approximation, the production and loss rates are equal and then from the count rates of the precursor ions [$O_2{}^+$] and of the product ions [$H_2O_2{}^+$], the fraction of H_2O_2 to H_2O in the helium, 2.8:97.2%, and the rate coefficient for reaction (4), i.e., k_4, the rate coefficient for reaction (6), i.e., k_6, can be determined from:

$$[O_2{}^+]\, k_4\, 2.8 = [H_2O_2{}^+]\, k_6\, 97.2 \quad (7)$$

Thus, k_6 is determined from the data given in Fig. 4a as $3.1 \times 10^{-9}\,cm^3\,s^{-1}$ at 300 K, which is effectively equal to the collisional rate coefficient calculated to be $3.2 \times 10^{-9}\,cm^3\,s^{-1}$ [24]. This is in accordance with the established rule, that exothermic proton transfer reactions invariably proceed at the collisional rate [28]. Note, however, that this value is greater than the value of 1.7×10^{-9} reported previously [9].

3.1.3. NO^+ reactions

Ground state NO^+ ions react slowly with H_2O molecules via three-body association:

$$NO^+ + H_2O + He \rightarrow NO^+H_2O + He \quad (8)$$

This is a key association reaction in ionospheric ion chemistry (but with N_2 and O_2 rather than He as the stabilising third bodies) that initiates the production of hydrated hydronium ions in the D-region [23]. The rate coefficient of reaction (8) is known to be $3.6 \times 10^{-29}\,cm^6\,s^{-1}$ at 300 K [21]. Repeating the experiments described above for $O_2{}^+$ ions using injected NO^+ ions and water vapour only reveals, as expected, product ions at m/z values of 48 and 66, these being $NO^+(H_2O)$ and $NO^+(H_2O)_2$. Introduction of the water vapour/hydrogen peroxide mixture into the carrier gas results in an additional product ion at m/z of 64, which must be $NO^+H_2O_2$. There is no indication that the $NO^+(H_2O_2)_2$ dihydrate ion is formed. The challenge now is to determine the route or routes to the production of $NO^+H_2O_2$ ions. There are two likely reactions, which are:

$$NO^+ + H_2O_2 + He \rightarrow NO^+H_2O_2 + He \quad (9)$$

$$NO^+H_2O + H_2O_2 \rightarrow NO^+H_2O_2 + H_2O \quad (10)$$

The three-body association reaction (9) is analogous to reaction (8). Ligand switching reactions like (10) are known to occur at or near the collisional rate when they are appreciably exothermic [21], but we cannot be certain that reaction (10) is exothermic, since no thermochemical data on the $NO^+H_2O_2$ ion are available. We can only obtain insight into these reactions from careful experimentation and a combination of the results from a parallel study of the reactions of NO^+ with water vapour and with the water vapour/hydrogen peroxide gas as we now describe. First, we consider the NO^+/H_2O reaction.

It is known that reaction (8) is very slow and so a SIFT measurement of its reaction rate coefficient, k_8, is not trivial, especially when the reactant neutral is a condensable vapour. But the association reaction (1) is faster, and therefore easier to measure. Indeed, its rate coefficient has been measured many times

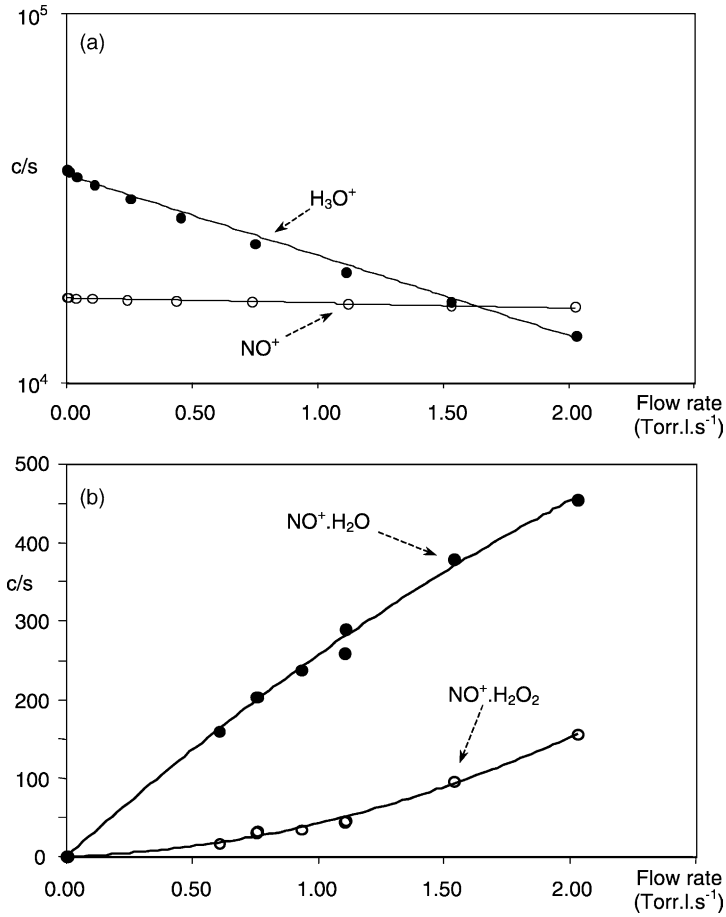

Fig. 5. (a) Decay plots of the count rates (c/s) of H_3O^+ and NO^+ ions simultaneously injected into the helium carrier gas of the SIFT against the flow rate (Torr L s^{-1}) of air/pure water headspace. The relative slopes of these decay plots provide the relative rate coefficients for the H_3O^+ and NO^+ reactions with water vapour, k_1 and k_8, respectively. Since k_1 is known [21], k_8 can be obtained. Note the much slower decay of the NO^+ ions, indicating that $k_8 \ll k_1$ (see text). (b) Count rates of the product ions of the NO^+ reactions with H_2O and H_2O_2, i.e., NO^+H_2O and $NO^+H_2O_2$, respectively, in counts per second, plotted as a function of flow rate (Torr L s^{-1}) of the air/water vapour/hydrogen peroxide headspace mixture. Fitting of these data to a simple kinetic model provides the rate coefficients for reactions (8)–(10) (see text for further discussion).

previously as $k_1 = 7 \times 10^{-28}$ cm^6 s^{-1} at 300 K [21]. The simplest approach to the measurement of k_8 is to inject H_3O^+ and NO^+ ions simultaneously into the helium carrier gas of the SIFT and then measure the decay rates of both these ion species as water vapour is introduced in the usual way. Typical decay curves are shown in Fig. 5a. Note the much slower decay of the NO^+ ions, which indicates that $k_8 \ll k_1$. Since k_1 is known, k_8 is simply determined from the ratio of these decay rates. Thus, k_8 is obtained as 3.6×10^{-29} cm^6 s^{-1} (at 300 K) which is in good agreement with the previous measurement [21]. As mentioned above, the dihydrate ion $NO^+(H_2O)_2$ is also formed, presumably via a secondary three-body reaction between NO^+H_2O ions and H_2O molecules. The relative signal level of the NO^+H_2O and $NO^+(H_2O)_2$ ions suggests that this secondary reaction proceeds faster than reaction (8), but further experiments need to be performed to derive its rate coefficient.

Experiments were then carried out to study the reaction of NO^+ ions with H_2O_2 in an attempt to ascertain which of reactions (9) and (10) resulted in the production of the $NO^+H_2O_2$ ions. Thus, NO^+ ions were injected into the helium carrier gas and controlled and measured amounts of the water vapour/peroxide headspace mixture were introduced via a flow controller. The decay of the precursor NO^+ ions even for the maximum flow of the reactant mixture was very small, which indicated that reaction (9) is also very slow and its rate coefficient cannot be accurately determined from the slope of the decay curve. So we resorted to accurately measuring the appearance of the product ions NO^+H_2O formed in reaction (8) and the $NO^+H_2O_2$ ions formed by either/or reactions (9) and (10). Typical data obtained are shown in Fig. 5b, where it can be seen that the signal level of the NO^+H_2O ions increase more rapidly than that of the $NO^+H_2O_2$ ions, by virtue of the greater fraction of H_2O in the water vapour/hydrogen peroxide headspace mixture. Further to this, the NO^+H_2O signal plot curves downwards at higher reactant flows, indicating that a loss process in addition to a formation process for these ions is occurring. This down curving is mirrored by an up curving of the $NO^+H_2O_2$ signal plot, which strongly implies that NO^+H_2O ions are being converted to $NO^+H_2O_2$ ions. This must be due to the switching reaction (10). However, this does not rule out parallel production of $NO^+H_2O_2$ ions by the association reaction (9).

In order to determine, the separate contributions of reactions (9) and (10) to $NO^+H_2O_2$ production, we resort to a simple kinetic model and apply it to the kinetic data given in Fig. 5b. Thus, using square brackets to indicate signal levels and neutral particle number densities, including the helium carrier gas [He], $[NO^+H_2O_2]$ is given by:

$$[NO^+H_2O_2] = [NO^+][H_2O_2]k_9[He]^{-1}t + \tfrac{1}{2}[NO^+] \times [H_2O]k_8[He]^{-1}t[H_2O_2]k_{10}$$

k_8 and k_9 are the three-body rate coefficients for reactions (8) and (9), k_{10} is the bimolecular rate coefficient for reaction (10) and t is the reaction time. The factor of 2 is included as an adjustment to the reaction time (i.e., $t/2$) for the secondary reaction (10) accounting for the continuous formation of the reacting secondary ions [29]. Using curve fitting, the values $k_9 = 3.8 \times 10^{-29}\,cm^6\,s^{-1}$ and $k_{10} = 2.5 \times 10^{-10}\,cm^3\,s^{-1}$ are obtained using the partial pressures of H_2O and H_2O_2 in the headspace mixture given previously (see Fig. 1).

It is interesting to note that k_9 is not measurably different than k_8 when the uncertainties in determining k_8 are considered. Our value of k_{10} is about factor of two greater than the estimate ($\sim 1 \times 10^{-10}\,cm^3\,s^{-1}$) made previously by others [9]. This means that when the sample vapour is rich in water vapour relative to hydrogen peroxide the relatively rapid switching reaction (10) is the major route to the production of $NO^+H_2O_2$ ions. Hence, the presence of the water vapour catalyses the production of $NO^+H_2O_2$ ions. That this switching reaction occurs implies that the binding energy of H_2O_2 to NO^+ ions exceeds that of H_2O (which is known to be $69.5\,kJ\,mol^{-1} = 0.72\,eV$ [30]). However, when switching reactions are appreciably exothermic they are known to proceed at or near to the collisional rate, but k_{10} falls well short of the collisional rate coefficient for this reaction, which is $3.0 \times 10^{-9}\,cm^3\,s^{-1}$ [24]. These data collectively imply that the difference between the binding energies of NO^+ to H_2O and of NO^+ to H_2O_2 is small. Thus, it might be expected that the reverse of reaction (10) may occur at the relatively high $[H_2O]/[H_2O_2]$ ratios of this experiment and that ultimately equilibrium could be established. But there is no evidence for this in the data shown in Fig. 5b, where it can be seen that the $NO^+H_2O_2/NO^+H_2O$ signal ratio increases continuously with increasing sample flow rate (i.e., increasing $[H_2O]$ and $[H_2O_2]$). The k values for these reactions are included in Table 1.

3.2. Peroxyacetic acid

We were unable to obtain pure peroxyacetic acid and so for these experiments we used a mixture comprising 40% peroxyacetic acid and 60% acetic acid by weight (Sigma-Aldrich Co.), although the suppliers' specification indicates that hydrogen peroxide is a

Table 1
Rate coefficients for the reactions of H_3O^+, NO^+ and O_2^+ with hydrogen peroxide and peroxyacetic acid

Molecule	α[a] (10^{-24} cm^3)	μ[a] (D)	H_3O^+[b]			NO^+[b]			O_2^+[b]		
			Product	k	k_c	Product	k	k_c	Product	k	k_c
Hydrogen peroxide	*2.9 ± 0.5*	2.2	–	–[c]	3.2	$NO^+H_2O_2$ (100)	–[d]	2.8	$H_2O_2^+$ (100)	2.0	2.7
Peroxyacetic acid	*5.5 ± 1.0*	*2.4 ± 0.3*	$CH_3COOH.H^+$ (90)	3.2	3.2	NO_2^+ (70)	1.7	2.7	$C_2H_4O_2^+$ (70)	2.7	2.7
			$CH_3C(O)OOHH^+$ (10)			$C_2H_3O^+$ (25) $NO^+CH_3(O)OOH$ (5)			$C_2H_3O^+$ (30)		

Also given are their polarisabilities, α, in units of 10^{-24} cm^3 and their permanent dipole moments, μ, in Debye (D). The collisional rate coefficients, k_c, calculated using the parameterised trajectory formulation of Su and Chesnavich [24], are given in square brackets. The product ions for the reactions and their percentage (in parentheses) are also indicated.

[a] The known μ value [25] is shown in regular type. The estimated α and μ are shown in italics.

[b] The rate coefficients, k, are in units of 10^{-9} cm^3 s^{-1}, for the NO^+ and O_2^+ reactions are experimentally derived (see the text). The absolute and relative uncertainties in these calculated rate coefficients are ±30 and ±15%, respectively.

[c] H_3O^+ does not react at a measurable rate with H_2O_2.

[d] Three body association $k_9 = 3.8 \times 10^{-29}$ cm^6 s^{-1}.

minor contaminant. The headspace concentrations of the separate components will not be in the same proportions as those in the liquid phase, but it is known that peroxyacetic acid is more volatile from water solution than acetic acid [31]. We show later that we can infer the relative headspace concentrations of these two compounds from the present ion chemistry study and it turns out that the headspace comprises 52% peroxyacetic acid and 48% acetic acid at room temperature. That these compounds are at comparable concentrations eases the determination of the peroxyacetic acid kinetics (contrast this with the water/hydrogen peroxide mixture described above). The reactions of H_3O^+, NO^+ and O_2^+ with acetic acid have been studied previously in our SIFT surveys of reactions relevant to SIFT-MS work [11], which allows the peroxyacetic acid kinetics to be extracted from the SIFT data obtained using the acetic/peroxyacetic acid mixture as the reactant. These experiments were carried out using the bag sampling method (at room temperature) described in Section 2.

The first step is to determine the rate coefficients for the reactions of the H_3O^+, NO^+ and O_2^+ ions with the reactant gases/vapours. To obtain the rate coefficients for the peroxyacetic acid reactions it was first necessary to obtain decay curves for a dry air/acetic acid mixture prior to using the dry air/acetic acid/peroxyacetic acid mixture. The three precursor ions were injected simultaneously into the helium carrier gas and the dry air/acetic acid mixture was introduced at measured flow rates. Typical ion decay curves obtained are shown in Fig. 6a. These curves show, as is known from our previous measurements [11], that the H_3O^+ and O_2^+ reactions proceed at their collisional rates, k_c, and that the NO^+ reaction is slower, actually proceeding with a rate coefficient of $0.4\,k_c$ at 0.5 Torr of helium [11]. This procedure was then immediately repeated using the air/acid mixture and sample decay curves obtained are shown in Fig. 6b. It is apparent again, that the H_3O^+ and O_2^+ reactions with the mixture of the two acid reactants are fast and this implies that both the H_3O^+ and O_2^+ reactions with peroxyacetic acid proceed at their respective collisional rates. The rate coefficients can be calculated if the polarisabilities and dipole moments of the acid molecules are known or can be estimated [24]. These parameters are known for acetic acid and so the k_c values for the acetic acid reactions can be readily calculated [24]. It has been necessary to estimate these parameters for peroxyacetic acid by analogy with similar compounds. Thus, the estimated k_c values for the peroxyacetic acid reactions are also given in Table 1. It is clear in Fig. 6b

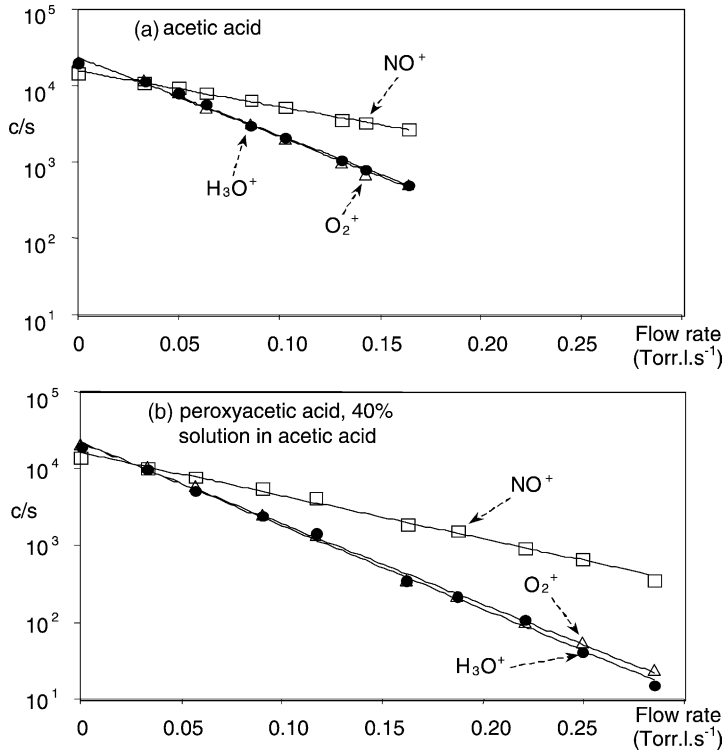

Fig. 6. Semilogarithmic plots of the count rates (c/s) against flow rate (Torr L s^{-1}) of H_3O^+, NO^+ and O_2^+ ions as a dilute mixture of (a) dry air/acetic acid and (b) dry air/peroxyacetic acid/acetic acid mixture is introduced into the helium carrier gas of the SIFT. The rate coefficients for the H_3O^+ reactions are assumed to be the respective collisional rate coefficients, k_c [24]. The derived rate coefficients for the NO^+ and O_2^+ reactions with acetic acid obtained from the relative slopes of the decay plots as in (a) agree with the previous measurements [11]. The rate coefficients for peroxyacetic acid reactions are calculated using the relative decay slopes from (b) considering the fractions of acetic acid and peroxyacetic acid in the gas phase (48:52%).

that the overall reaction of NO^+ with the mixture of acid vapours is relatively slow. By combining the data from Fig. 6a and b and the fractions of acetic and peroxyacetic acid in the reactant mixture, the rate coefficient for the NO^+ reaction with peroxyacetic acid is obtained as 1.7×10^{-9} cm^3 s^{-1}, which is equal to $0.6\,k_c$.

3.2.1. H_3O^+ reactions

It is known that H_3O^+ reacts with acetic acid via non-dissociative proton transfer producing only CH_3COOHH^+ ions at a *m*/*z* value of 61 [11]. So it is no surprise that ions at this *m*/*z* appear on the product ion spectrum when the acetic acid/peroxyacetic acid mixture is the reactant. However, the only other product ion that appears is a minority ion at *m*/*z* of 77, which is surely protonated peroxyacetic acid, $CH_3C(O)OOHH^+$. The data indicate that the peroxyacetic acid reaction proceeds thus:

$$H_3O^+ + CH_3C(O)OOH \rightarrow CH_3C(O)OOHH^+ + H_2O \quad (10\%) \qquad (11a)$$

$$H_3O^+ + CH_3C(O)OOH \rightarrow CH_3COOHH^+ + H_2O_2 \quad (90\%) \qquad (11b)$$

Using the relative signal levels at *m*/*z* values of 61 and 77 together with the relative number densities of acetic acid and peroxyacetic acid in the helium carrier gas (and using the rate coefficients for these two

reactions; see Table 1), the product distribution for reaction (11) is obtained, as indicated. Thus, reaction (11b) is the dominant reaction pathway. This is a curious reaction in which it seems that intermediate $\{H_3O^+CH_3C(O)OOH\}$ ion complexes are formed from which ($H_2O + O$) and, less frequently, H_2O molecules are lost. Although direct proton transfer must be exothermic in view of the rapidity of the reaction, and the occurrence of reaction (11a), it is unlikely that the protonated molecule can spontaneously lose an oxygen atom and so the neutral product of reaction (11b) is most likely to be H_2O_2. Unfortunately, the heat of formation of peroxyacetic acid is not tabulated, but we can use the fact that a mixture of peroxyacetic acid (15%), water (40%), acetic acid (30%) and hydrogen peroxide (15%) exists in equilibrium [7] to estimate heat of formation of $CH_3C(O)OOH$ as $\sim(-320 \pm 5)$ kJ mol^{-1}. Using this value, the exothermicity of reaction (11b) is 105 kJ mol^{-1}, but to produce $H_2O + O$ it would be 40 kJ mol^{-1} endothermic. Occurrence of reaction (11a) at thermal energy (300 K) indicates that the proton affinity of peroxyacetic acid exceeds that of water, which is 691 kJ mol^{-1} [20].

3.2.2. O_2^+ reaction

Our previous SIFT study showed that O_2^+ reacts with acetic acid to produce CH_3CO^+ (50%) and the parent cation CH_3COOH^+ (50%) [11]. The present studies showed that only product ions at *m*/*z* values of 43 and 60 were formed when the acetic acid/peroxyacetic acid was used as the reactant neutral. Thus, it is clear that the product ions for the reaction of O_2^+ with peroxyacetic acid are the same *m*/*z* values as those for the O_2^+/acetic acid reaction, so the former reaction proceeds thus:

$$O_2^+ + CH_3C(O)OOH \rightarrow C_2H_4O_2^+ + (O + O_2) \quad (70\%) \tag{12a}$$

$$O_2^+ + CH_3C(O)OOH \rightarrow CH_3CO^+ + HO_2 + O_2 \quad (30\%) \tag{12b}$$

Again, the product distribution indicated is obtained by considering the known distribution for acetic acid and the relative signal levels of the product ions at *m*/*z* values of 43 and 60 when the acid mixture is used as the reactant. We cannot definitely identify either the structure of the product ion of reaction (12a) or the neutral products of these reactions. But it is most probable that the reaction proceeds via dissociative charge transfer (in common with most O_2^+ reactions [11,13,14,21]) producing neutral O_2 molecules in both channels, this being surely so for reaction (12b). Using our estimated heat of formation of $CH_3C(O)OOH$ given above, we can calculate that reaction (12a) is thermoneutral for the CH_3COOH^+ structure of the product ion but exothermic by 92 kJ mol^{-1} for the $CH_2C(OH)_2^+$ structure of the product ion. Reaction (12b) is exothermic by 182 kJ mol^{-1}.

3.2.3. NO^+ reactions

The reaction of NO^+ with acetic acid produces only the adduct NO^+CH_3COOH ion at an *m*/*z* value of 90 [11]. Use of the acid mixture as the reactant resulted in three additional ions at *m*/*z* values of 43, 46 and 106. The last is only a minor product and must surely be the adduct $NO^+CH_3C(O)OOH$ ion and the first must be CH_3CO^+. There is only one reasonable candidate for the product ion at the *m*/*z* value of 46, viz. NO_2^+. To check if this ion contained a carbon atom (it could conceivably have a molecular formula of CH_4NO^+ [20]) we carried out an isotope check by measuring the ratio of the signal levels at *m*/*z* values of 46 and 47 (the ^{13}C isotopomer). No significant signal was observed at *m*/*z* 47, showing that the product ion does not contain a carbon atom and therefore must be NO_2^+. So the reaction proceeds thus:

$$NO^+ + CH_3C(O)OOH \rightarrow NO^+CH_3C(O)OOH \quad (5\%) \tag{13a}$$

$$NO^+ + CH_3C(O)OOH \rightarrow NO_2^+ + CH_3COOH \quad (70\%) \tag{13b}$$

$$NO^+ + CH_3C(O)OOH \rightarrow CH_3CO^+ + HNO_3 \quad (25\%) \tag{13c}$$

It is fortunate that none of these product ions result from the NO^+/acetic acid reaction. So the relative

signal level at the *m*/*z* value of 90 and the total signal level of the ions at *m*/*z* values of 43, 46 and 106, together with the rate coefficients for the NO^+ reactions with acetic and peroxyacetic acids (given in Table 1), provide the relative headspace concentrations of these acids in the headspace of the liquid acid mixture. This is how the 48 and 52% composition (partial pressure ratio) given above was obtained.

This complex reaction probably proceeds via the formation of the adduct ion indicated in reaction (13a), which then largely dissociates along the two product channels indicated as reactions (13b) and (13c). That the overall reaction proceeds more slowly than the collisional rate, like that for the NO^+/acetic acid reaction, gives some credence to this hypothesis. But, of course, the major reaction (13b) can be viewed as an oxygen atom abstraction reaction that results in the oxidation of NO^+ ions to $NO_2{}^+$ ions and, similarly, reaction (13c) may be viewed as HO_2 molecule abstraction. In the latter reaction, the structure of the neutral product is unknown; it could be either a nitric acid molecule, as written, or the peroxynitrous acid HOONO isomer [32]. Using our estimated heat of formation of peroxyacetic acid of $-320\,kJ\,mol^{-1}$, reaction (13b) is exothermic by $122\,kJ\,mol^{-1}$ and reaction (13c) is exothermic by $146\,kJ\,mol^{-1}$ with HNO_3 as a neutral product.

4. Concluding remarks

The experimental challenge in this study has centred on the fact that neither hydrogen peroxide nor peroxyacetic acid could be obtained in total isolation from water and acetic acid, respectively. Hence, the rate coefficients and product ion distributions for their reactions had to be extracted from the reactions of the respective mixtures. This has required careful ion chemical modelling in order to obtain the kinetic data for the hydrogen peroxide reactions. However, it should be noted when attempting to analyse hydrogen peroxides in atmospheric air that water vapour will inevitably be present in greater concentrations and so the challenge has to be met. Similarly, acetic acid inevitably will be present when peroxyacetic acid is to be analysed in air.

The initial stimulus for this study was to investigate the potential of SIFT-MS for the analysis of these peroxides in air and exhaled breath using the three most common precursor ions H_3O^+, NO^+ and $O_2{}^+$. It is clear that both H_3O^+ and $O_2{}^+$ precursor ions are of little value for such analyses. H_3O^+ does not react with H_2O_2 and the $O_2{}^+$ reaction produces $H_2O_2{}^+$ ions that react rapidly with H_2O molecules. Peroxyacetic acid reacts with H_3O^+ and $O_2{}^+$ ions to produce ions that are common with those of the analogous acetic acid reactions. Fortunately, however, NO^+ is revealed as a suitable ion for the analyses of these two peroxides. $NO^+H_2O_2$ ions are formed when water/hydrogen peroxide molecules react with NO^+ ions, the formation of $NO^+H_2O_2$ ions being catalysed by the presence of water molecules. For the analysis of peroxyacetic acid in the presence of acetic acid, $NO_2{}^+$ ions are revealed as suitable monitor ions for SIFT-MS analyses using NO^+ precursor ions. Thus, it is now possible to use SIFT-MS to monitor peroxyacetic acid in the industrial environment where it is used for disinfection and bleaching. It is possible that a precursor negative ion species such as CF_3O^- may be a more suitable chemical ionisation agent for these peroxides, but negative ions have not yet been utilised for our SIFT-MS work.

Acknowledgements

We thank the reviewer of this paper for his/her constructive comments. We thank Edward Hall for his assistance with the experiments and John Cocker for helpful discussions. We gratefully acknowledge financial support by the Engineering and Physical Sciences Research Council, UK (grant reference GR/M89195/01) and the Grant Agency of the Czech Republic (project numbers 202/03/0827 and 203/02/0737).

References

[1] C.A. Schalley, R. Wesendrup, D. Schröder, H. Schwarz, Organometallics 15 (1996) 678.

[2] A.W. Dohlman, H.R. Black, J.A. Royall, Am. Rev. Respir. Dis. 148 (1993) 955.
[3] P. Latzin, M. Griese, Eur. J. Med. Res. 7 (2002) 353.
[4] M.G.C. Baldry, J. Appl. Bacteriol. 54 (1983) 417.
[5] H.I. Feldman, M. Kinosian, W.B. Bilker, C. Simmons, J.H. Holmes, M.V. Pauly, J.J. Escarce, J. Am. Med. Assoc. 276 (1996) 620.
[6] L.B. Brasileiro, J.L. Colodette, D. Pilo-Veloso, Quimica Nova 24 (2001) 819.
[7] P.A.A. Solvay Team, Oxymaster® 15 Datasheet, Solvay S.A., Warrington, UK, 2001.
[8] F. Gagnaire, B. Marignac, G. Hecht, M. Hery, Ann. Occup. Hyg. 46 (2002) 97.
[9] W. Lindinger, D.L. Albritton, C.J. Howard, F.C. Fehsenfeld, E.E. Ferguson, J. Chem. Phys. 63 (1975) 5220.
[10] D. Smith, P. Španěl, Rapid Commun. Mass Spectrom. 15 (2001) 563.
[11] P. Španěl, D. Smith, Int. J. Mass Spectrom. Ion Process. 172 (1998) 137.
[12] D. Smith, N.G. Adams, Adv. Atom. Mol. Phys. 24 (1987) 1.
[13] P. Španěl, D. Smith, Int. J. Mass Spectrom. Ion Process. 167/168 (1997) 375.
[14] P. Španěl, J.M. van Doren, D. Smith, Int. J. Mass Spectrom. 213 (2002) 163.
[15] P. Španěl, D. Smith, Med. Biol. Eng. Comput. 34 (1996) 409.
[16] T. Wang, D. Smith, P. Španěl, Rapid Commun. Mass Spectrom. 16 (2002) 1860.
[17] P. Španěl, A.M. Diskin, S.M. Abbott, T. Wang, D. Smith, Rapid Commun. Mass Spectrom. 16 (2002) 2148.
[18] J.J. van Laar, Z. Physik. Chem. 72 (1910) 723.
[19] V.M. Bierbaum, M.F. Golde, F.J. Kaufman, Chem. Phys. 65 (1976) 2715.
[20] E.P. Hunter, S.G. Lias, in: W.G. Mallard, P.J. Linstrom (Eds.), Proton Affinity Evaluation in NIST Chemistry WebBook, NIST Standard Reference Database Number 69, February 2000, National Institute of Standards and Technology, Gaithersburg, MD, 20899.
[21] Y. Ikezoe, S. Matsuoka, M. Takebe, A. Viggiano, Gas Phase Ion–Molecule Reaction Rate Constants Through 1986, Maruzen, Tokyo, 1987.
[22] S.G. Lias, in: W.G. Mallard, P.J. Linstrom (Eds.), Ionization Energy Evaluation in NIST Chemistry WebBook, NIST Standard Reference Database Number 69, February 2000, National Institute of Standards and Technology, Gaithersburg, MD, 20899.
[23] E.E. Fergusson, F.C. Fehsenfeld, D.L. Albriton, in: M.T. Bowers (Ed.), Gas Phase Ion Chemistry, Academic Press, New York, 1979, p. 45.
[24] T. Su, W.J. Chesnavich, J. Chem. Phys. 76 (1982) 5183.
[25] D.R. Lide (Ed.), CRC Handbook of Chemistry and Physics, CRC, Boca Raton, 1991.
[26] D. Smith, N.G. Adams, in: M.A. Almoster Ferreira (Ed.), NATO Advanced Study Institute on Chemistry of Ions in the Gas Phase, Vimeiro, Portugal, Reidel, 1984, p. 41.
[27] W. Li, B. Ni, D. Jin, Q. Zhang, Chin. Sci. Bull. 33 (1988) 1610.
[28] G. Bouchoux, J.Y. Salpin, D. Leblanc, Int. J. Mass Spectrom. Ion Process. 153 (1996) 37.
[29] P. Španěl, D. Smith, Rapid Commun. Mass Spectrom. 14 (2000) 1898.
[30] J.S. Francisco, J. Chem. Phys. 115 (2001) 2117–2122.
[31] R. Sander, Henry's Law Constants, in: P.J. Linstrom, W.G. Mallard (Eds.), NIST Chemistry WebBook, NIST Standard Reference Database Number 69, July 2001, National Institute of Standards and Technology, Gaithersburg, MD, 20899.
[32] W.A. Pryor, G.L. Squadrito, Am. J. Physiol. 268 (1995) L699.